The Design, Development and Qualification of a Lightweight Antenna Pointing Mechanism

M. Shmulevitz* and A. Halsband*

Abstract

This paper describes the design, development, and qualification of a new lightweight and compact Antenna Pointing Mechanism (APM). The APM was specially designed to meet the stringent mass, envelope, and environmental requirements of OFFEQ experimental satellite. During the development phase, some problems were encountered with the brushless DC motors, slip ring contact resistance, and bearing drag torque. All of these problems were resolved, and two APM units have been operating successfully in orbit since April, 1995.

Introduction

Data link between OFFEQ experimental satellite and ground control is provided by two redundant APM units. The strict and demanding requirements for minimum mass and envelope enhanced a unique design approach featuring a lightweight (1.8 kg) and compact (150-mm flange diameter x 220-mm length) antenna pointing mechanism.

Although the APM housings and shafts were manufactured from aluminum alloy, the overall system design allows a large temperature range (-30°C to +60°C) without any active thermal control. Based on a gimbal (pitch over yaw) arrangement, the mechanism has hard-preloaded ball bearings and aluminum gears lubricated with sputtered MoS_2. The APM is designed for LEO applications and configured to minimize effects of monatomic oxygen erosion on the tribological elements. Electrical transfer (command & power) to the elevation axis is achieved by a compact slip ring unit, and RF feed to the antenna is accomplished via two miniature rotary joints. The APM has been tested in thermal vacuum conditions to a 4-year equivalent life in orbit. Its overall pointing accuracy is 1°, and the average power consumption is 2 watts.

During the development phase, some problems were encountered with the brushless DC motors, slip ring unit, and bearing drag torque. Changing the materials in the motor resolved the cracks and cuts that formed in the windings. The slip ring unit exhibited increased electrical resistance after exposure to laboratory air. Rotation for a only few revolutions restored normal conditions. In order to reduce blocking effects, the APM bearings contain toroid ball separators and "loose" conformity races. However, this approach did not eliminate the increase of drag torque encountered during the life test. Also, it has been found that a dependency, which was stabilized at an acceptable torque margin, exists between APM mode of operation and drag torque.

---

* Israel Aircraft Industries / MBT, Yehud, Israel

APM Description

The APM (Figures 1 and 2) provides more than a full hemispherical coverage due to its capability to rotate continuously in the azimuth axis and to its 0°-115° rotation range in the elevation axis. The APM azimuth axis consists of a rotating inner housing that is simply supported by a pair of bearings: the large bearing is fixed, and the small bearing floats with respect to the stationary housing. The bearings used for this application were 440C stainless steel, precision (ABEC 7) angular-contact ball bearings (bore diameters 58.73 mm and 19.05 mm, respectively) with double rows of balls, preloaded back-to-back, and protected by two metal shields. Only the grooves were dry-lubricated with sputtered MoS_2, and ball separators were toroid rings made of Duroid.

The rotating assembly is driven by a brushless DC motor via a stainless steel spur gear that meshes with a gear made of aluminum alloy and lubricated with sputtered MoS_2 (same for all other gears in the mechanism). The servo control feedback is provided by a resolver and aluminum gear mesh. To enable the continuous azimuth rotation, electrical and RF transfers to the elevation axis are achieved by a slip ring unit and rotary joint, respectively.

The elevation axis of the APM consists of two rotating arms: one is axially fixed, and the other arm floats axially with respect to the inner housing. A brushless DC motor drives the axially fixed arm, whereas the elevation resolver (not seen in the cross-section of Figure 2) is driven by the floating arm via an aluminum gear mesh. RF transfer to the antenna is accomplished with the elevation rotary joint and coaxial cables. The hold down and release mechanism, attached to the antenna backside tip, provides the stowage and release capability. The antenna itself consists of a printed circuit board made of Duroid and is bonded to a honeycomb sandwich with high-modulus, graphite-epoxy face sheets.

Design Philosophy

The APM design approach focused on one main objective: to minimize the APM mass, yet withstand all other requirements, as defined in Table 1. A compact design and selection of proper materials were considered the method to obtain the design goals.

The selection of materials started with titanium alloy as the first choice for the APM shaft and housing material. It has the advantage of a coefficient of thermal expansion (CTE) that closely matches the selected 440C stainless steel bearing material and a good stiffness-to-weight ratio. However, careful examination of the APM mass budget revealed that, with titanium alloy, the allocated overall mass will be exceeded. Beryllium and other exotic materials were considered unfavorable due to fabrication problems, availability, and price. Aluminum alloy (7075-T7351) was the second choice to be checked. With respect to APM mass budget and stiffness-to-weight ratio, aluminum alloy is a good choice. But with the big difference in CTE between aluminum alloy and 440C stainless steel, this solution seemed unacceptable.

Nevertheless, a thorough investigation has been carried out and, with the assistance of the European Space Tribology Laboratory (ESTL) computer prediction, bearing frictional torque and contact stress were analyzed as a function of different bearing fits and thermal strains. The results showed that, although there is a large increase in bearing frictional torque and contact stress, the obtained values are still acceptable. The nominal frictional torque of the whole system was specified to be 10% of motor stall torque at ambient conditions, and the servo control was designed to accommodate the large change in friction torque. The most significant result of this analysis was the understanding of mechanism performance as a function of thermal gradients. With a hard preloaded back-to-back bearing arrangement and aluminum shaft and housing, bearing torque and contact stress increase rapidly when the outer bearing race temperature is lower than the inner race temperature. The opposite will occur if the outer bearing race temperature is higher than the inner race temperature. In that case, for only a 10°C temperature gradient, the bearings will be off-loaded (i.e., no preload). System design of OFFEQ satellite required direct installation (i.e., no booms) of the APM to the OFFEQ plate at the nadir side. Thermal analysis showed that, for most cases, the APM outer housing, which is attached to OFFEQ plate, will have higher temperatures with respect to the inner housing (shaft), which points to space. Therefore, the tendency is that thermal gradients will reduce bearing preload and friction torque. The worst condition will be an isothermal case with no gradients. In addition, tolerance analysis showed that, with a clearance fit and bearings off-loaded, the pointing accuracy and stiffness will not be adversely affected.

A considerable amount of work has been taken by our subcontractor to develop the rotary joint. The critical parameter of the rotary joint is the ability of the bearings to conduct the heat dissipated in the rotating section of the co-axial line to the housing. The thermal conductance of a ball bearing in vacuum is proportional to the axial and radial load, the size of the bearing, and the number and diameter of balls. A face-to-face bearing arrangement has been used to ensure that bearing thermal conductance increases when the temperature of the shaft rises above that of the housing. Also, a compliant spacer was used to compensate for the change in preload due to thermal gradients. To improve the thermal conductivity, all metallic parts, except for the bearings, were made from aluminum or beryllium copper.

Testing

The design and location of the APM antenna impose a large static imbalance with respect to the APM elevation and azimuth axes. In order to simulate correctly APM performance in orbit and to eliminate all G effects, the antenna has been replaced by a dummy payload for all functional and thermal vacuum tests. This dummy payload has the same inertial load and stiffness as the antenna, and its center of gravity coincides with the APM axes. The APM qualification model has been subjected to the following tests:

Functional tests - These tests have been performed during the various stages of APM qualification. They include static and dynamic pointing accuracy check, torque threshold at different angular positions, dynamic check, and RF test. Dynamic check was executed by operating the APM at a typical tracking mode for seven minutes. Current and voltage consumption were monitored, and system tracking error was derived by comparison of command versus resolver position.

Vibration tests - Vibrations were conducted with the APM stowed in the launch configuration. Three types of vibration tests were carried out: sine vibration (10g sinusoidal up to 200 Hz), random vibration (12.5 Grms up to 2000 Hz, 3 min per axis), and acoustic test (142 dB overall noise level, 3-min duration). The APM was also subjected to three shocks of 50g for 11 ms in each axis direction.

Thermal vacuum cycling - This test was conducted by exposing the APM to eight temperature cycles between -40°C to +60°C at a vacuum level of 10^{-6} Torr. At each of the temperature extremes, functional tests were carried out.

Thermal vacuum life test - This was an accelerated test divided into two phases. At phase 1, temperature condition was +23°C, whereas temperature condition was -20°C in phase 2 (vacuum was 10^{-6} Torr). In each phase of the test, the APM was operated in a typical tracking mode maneuver for seven minutes, then for two minutes. All the obtained data was processed and statistically analyzed. Having completed this basic cycle (7 minutes operation + 2 minutes processing), repeated cycles, to an equivalent life of two years in orbit, were carried out automatically by special software.

Problems Resolved

Slip ring contact resistance

During functional testing of the APM (vacuum, ambient temperature), unexpected dither behavior of the elevation axis was observed. Failure investigation revealed an excessive increase of contact resistance in the slip ring signal tracks (in the magnitude of hundreds and thousands of ohms). A short run-in (even two revolutions) was found to be sufficient to restore the slip ring contact resistance to its normal values. Yet, our main concern was the cause of slip ring contamination. It was believed that MoS_2 particles from the APM gears contaminated the slip ring, since MoS_2 has the property of semiconductor resistance.

A contamination barrier was introduced into the APM to prevent particles from falling on the slip ring tracks. However, dither behavior of the elevation axis still occurred whenever the APM was operated (in vacuum) after exposure to laboratory air. In addition, high contact resistance was also found in the slip ring power tracks, thus showing that at least 8 contact points are being contaminated simultaneously, and that did not seem reasonable. Further investigation with the slip ring manufacturer revealed that oxidation of the slip ring galvanic deposit may occur in air. It was also suggested that, for future application and new orders of slip rings, the galvatronics shall be coated with a 0.2-μm Au-Co layer, called DUOR, which acts as a dry lubricant and corrosion protection. Finally, it was decided that at the beginning of life in orbit, the APM will undergo a short run-in as a "cleaning process."

Brushless DC motor

During life testing at -20°C, a serious problem arose with the brushless DC motor. The phenomenon was a large increase in the input voltage without any change in the input current. Checking motor resistance revealed that the resistance is doubled, which indicates that there is a cut in the motor windings. It should be stated that this type of motor was a qualified item with space heritage.

The brushless DC motor basically consists of a ring-shaped stator with molded windings, a permanent magnet rotor without windings, and an inductive pick-off. A review of stator materials and manufacturing procedures revealed that cracks are usually formed in the epoxy resin, which is used for the impregnation of the windings. In addition, stress analysis showed that a cut will occur with a crack size of 0.02 mm. The failed motor was disassembled from the APM and dismantled into parts. Then, by thorough inspection of the stator, a cut beneath a crack of 0.04-mm width was found.

Subsequent efforts were taken by our vendor to qualify stators with various epoxy resins and to improve an insulation disc. These stators were subjected to endurance thermal tests, including 72 thermal shocks between -55°C to +115°C for a dwell time of 1 hour and transfer in 7 seconds. It was found that a rigid insulation disc of titanium alloy and scotchcast 281 epoxy resin gives the best results. Consequently, all motors were repaired to include these modifications.

Drag torque

APM drag torque is composed of its bearing, slip ring, rotary joint, and resolver torques. The most sensitive items that contribute to the overall drag torque are the bearings. In order to reduce blocking effects, the selected bearings contain toroid ball separators and "loose" conformity (56%) inner and outer races. During phase 1 of the life test at +23°C, APM voltage consumption, which is related to the drag torque, increased from 18 PWM to 28 PWM, where it was stabilized. The stall torque of the motor is 200 PWM, and therefore torque margin is high. The notch (Figure 3) is a result of a one-day intermission in the test. It indicates that the system has a relaxation property when not operated, but this phenomena is not well understood.

During phase 2 of the life test at -20°C, APM voltage and current consumption were considerably higher due to the thermal strain effects. Azimuth axis voltage consumption increased from 30 PWM to about 50 PWM, where it was stabilized at an acceptable torque margin. Performing a short run-in of the system showed that the overall drag torque was reduced. This behavior is attributed to the spread of debris piling and the "release" of cage wind up.

Conclusions

The design, development, and testing approaches were verified with the successful operation of two APM units in orbit. Satellite telemetry shows good correlation between the drag torque obtained during ground testing and the drag torque in orbit. Moreover, checking the drag torque with respect to the temperature of the OFFEQ plate indicates that the two APM units are exposed to thermal gradients that reduce the bearing preload and torque. It is of vital importance to consider the thermal environment and temperature during the conceptual design of any mechanism. Finally, although developed specifically for the OFFEQ satellite, the APM is a versatile design that may be adapted to other gimbal applications.
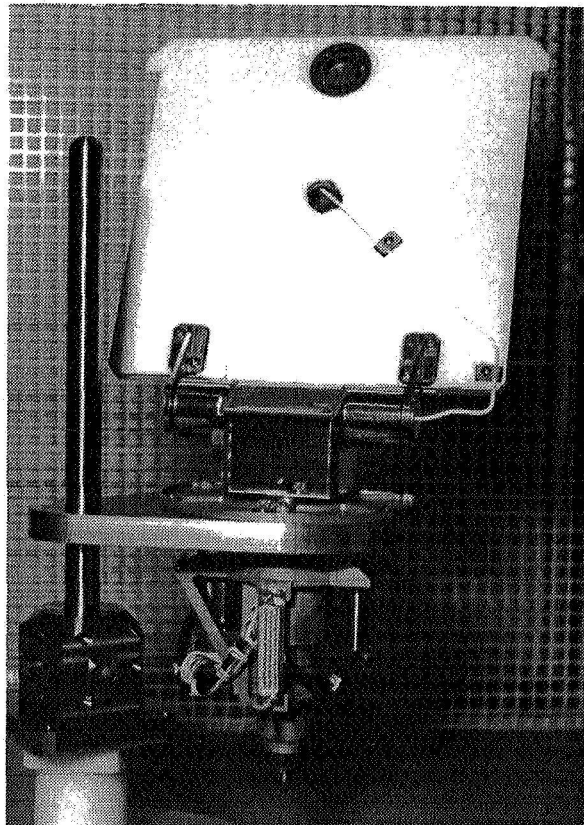
Acknowledgment

The authors wish to thank Dr. Rob Rowntree of ESTL for his consulting concerning the analysis of bearing frictional torque, contact stress, and tribology design. We also wish to thank the SAGEM team for their collaboration in solving the problem with the brushless DC motor and Eli Levy and Dov Varbin of MBT for their contribution to the development of the electronics and servo control.

References

1. T. A. Harris, Rolling Bearing Analysis, John Wiley and Sons, Inc., 1984.
2. S. H. Loewenthal, "Two Gimbal Bearing Case Studies: Some lessons learned," NASA 22nd Aerospace Mechanisms Symposium, May 1988, pp. 253-269.
3. ESTL, Tribology for Spacecraft, Course Notes.

Table 1. Main Requirements and Capabilities

Parameter		Requirement	Capability
Mass (payload excluded)	[Kg]	<2	1.8
Azimuth rotation	[deg]	±180	360 cont.
Elevation rotation	[deg]	0 - 115	0 - 115
Total pointing accuracy	[deg]	1.8	1.0
Max. angular acceleration	[deg/sec^2]	10	10
Max. angular velocity	[deg/sec]	10	10
Eigenfrequency	[Hz]	>50	250
Torsion stiffness	[N-m/rad]	>400	6500
Torque margin		>3.0	>5.5
Operating temperature	[°C]		
Maximum		+50	+60
Minimum		-20	-30
Mode of operation (tracking mode)		Intermittent	Obtained
Life	[years]	>2	4

Figure 1. APM Qualification Model
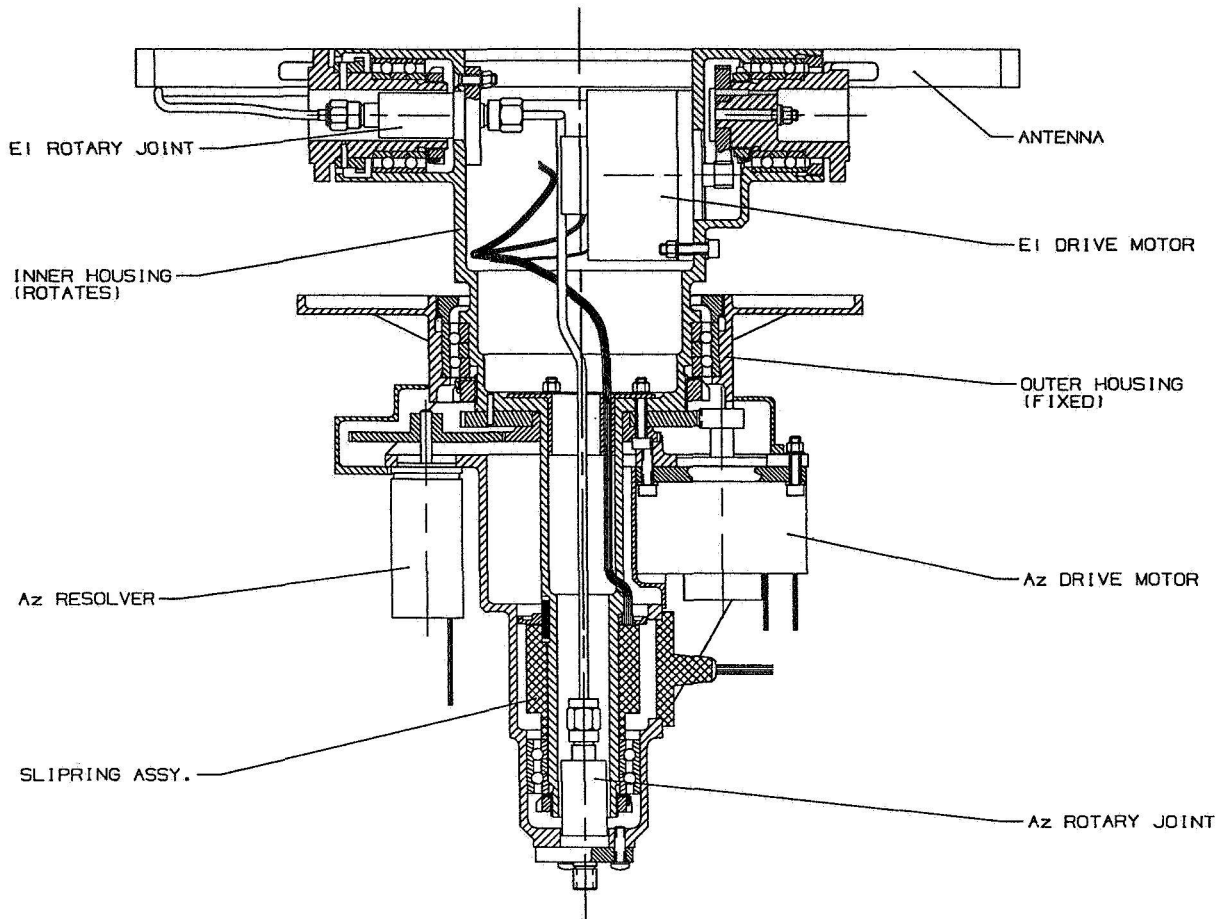
Figure 2. APM Cross Section

Labels (left side):
- EI ROTARY JOINT
- INNER HOUSING (ROTATES)
- Az RESOLVER
- SLIPRING ASSY.

Labels (right side):
- ANTENNA
- EI DRIVE MOTOR
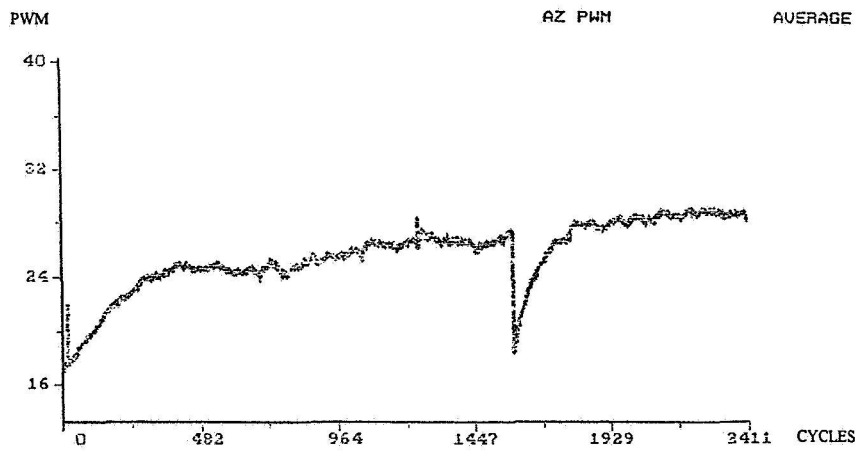- OUTER HOUSING (FIXED)
- Az DRIVE MOTOR
- Az ROTARY JOINT

Figure 3. Life Test - Phase 1, Voltage Consumption Summary